Biological Evaluation of Multiple Disulfide Cyclotide Scaffolds and Other Mimetics at Human Melanocortin Receptors

Author: Jennifer Bao
Project Advisor: Victor Hruby

A Thesis Submitted to the Department of Chemistry and Biochemistry and the Honors College in Partial Fulfillment of the Bachelors of Science Degree in Biochemistry with Honors

Department of Chemistry & Biochemistry
The University of Arizona
May 2013

Approved by:

Dr. Victor Hruby
Faculty Thesis Advisor

4/25/2013
Date

Dr. Megan McEvoy
Biochemistry Undergraduate Advisor

4/25/13
Date

The University of Arizona Electronic Theses and Dissertations
Reproduction and Distribution Rights Form

The UA Campus Repository supports the dissemination and preservation of scholarship produced by University of Arizona faculty, researchers, and students. The University Library, in collaboration with the Honors College, has established a collection in the UA Campus Repository to share, archive, and preserve undergraduate Honors theses.

Theses that are submitted to the UA Campus Repository are available for public view. Submission of your thesis to the Repository provides an opportunity for you to showcase your work to graduate schools and future employers. It also allows for your work to be accessed by others in your discipline, enabling you to contribute to the knowledge base in your field. Your signature on this consent form will determine whether your thesis is included in the repository.

Name (Last, First, Middle)

Bao, Jennifer, Margaret

Degree title (eg BA, BS, BSE, BSB, BFA):

B.S.

Honors area (eg Molecular and Cellular Biology, English, Studio Art):

Biochemistry; Biology (Biomedical Sciences Emphasis)

Date thesis submitted to Honors College:

04/26/2013.

Title of Honors thesis: Biological Evaluation of Multiple Disulfide Cyclotide Scaffolds and Other Mimetics at Human Melanocortin Receptors

The University of Arizona Library Release Agreement

I hereby grant to the University of Arizona Library the nonexclusive worldwide right to reproduce and distribute my dissertation or thesis and abstract (herein, the "licensed materials"), in whole or in part, in any and all media of distribution and in any format in existence now or developed in the future. I represent and warrant to the University of Arizona that the licensed materials are my original work, that I am the sole owner of all rights in and to the licensed materials, and that none of the licensed materials infringe or violate the rights of others. I further represent that I have obtained all necessary rights to permit the University of Arizona Library to reproduce and distribute any nonpublic third party software necessary to access, display, run or print my dissertation or thesis. I acknowledge that University of Arizona Library may elect not to distribute my dissertation or thesis in digital format if, in its reasonable judgment, it believes all such rights have not been secured.

☒ Yes, make my thesis available in the UA Campus Repository!

Student signature: _____ Date: 04/25/2013.

Thesis advisor signature: _____ Date: 04/25/2013.

☐ No, do not release my thesis to the UA Campus Repository.

Student signature: _____ Date: _____

Last updated: 04/01/13

Table of Contents

Abstract

Because of their multiplicity and ubiquity in mammalian systems as central modulators of signaling, GPCRs have held a special interest in drug design. Specifically, ligands targeting the homeostatic class of GPCRs known as melanocortin receptors (MCRs) have the potential to remedy the symptoms of obesity, diabetes, and pain. Adenylate cyclase and binding assays were performed on HEK 293 cells expressing hMC1R, hMC3R, hMC4R, and hMC5R to assess a class of 39 multiple-disulfide, cyclized MSH analogues featuring strategic *N*-methylation and based on the protein topology of conotoxins found in the venoms of marine cone snails. Because of their potency and selectivity, conotoxins offer a promising avenue for drug design; furthermore, the cyclic backbone and cystine knot motifs of the analogues afforded specific conformational constraining in addition to enhanced proteolytic stability and bioavailability. Several selective compounds were identified from the library with IC_{50} and EC_{50} values in the low nanomolar to low micromolar range; these results provide important starting points for optimization. Additionally, two libraries of small molecule mimetics and cyclic peptide analogues synthesized by former group members James Cain and Joel Nyberg were assessed using the same methods; therapeutically relevant selectivity profiles were exhibited by several small molecules in these libraries.

Introduction

G protein-coupled receptors (GPCRs), also known for their characteristic consensus structure as seven-transmembrane (7TM) domain receptors, are prevalent in eukaryotic organisms for their ability to induce intracellular signal transduction pathways as a result of extracellular stimuli. They constitute a myriad protein family of nearly 1000 membrane proteins encoded by over 800 genes in the human genome[1], and function primarily by small-scale conformational changes induced by the binding of small molecules, peptides, or proteins in the extracellular loops that constitute their orthosteric binding pocket[2]. Upon such conformational changes, heterotrimeric G proteins otherwise associated with these receptors unbind and separate into their constituent α- and βγ-subunits, which then diffuse freely across the plasma membrane to regulate the activity of enzymatic proteins and ion channels, ultimately influencing a change in the cell's activity[3].

GPCRs represent lucrative aims for the development and administration of novel drugs primarily because of their extensive presence and diversity in the human body, and currently constitute nearly 60% of modern drug targets[4]. More specifically, a class of GPCRs called melanocortin receptors have been identified and employed in the development of medicinal drugs pertinent to their central role in mammalian energy homeostasis, including their regulation of metabolism, immunity, exocrine gland secretion, inflammation, and feeding and sexual behavior[5]. Chemotherapeutic ligands targeting melanocortin receptors are therefore capable of remedying the symptoms of such diseases as obesity, anorexia, diabetes, and erectile dysfunction, all of which may occur as a result of impaired endogenous responses involving the central melanocortin system[6,7].

To date, there are five known human melanocortin receptors that have been applied in the development of pharmaceutical treatments for these and other diseases[8]; the focus of the Hruby laboratory rests primarily on four of the five members: hMC1R, hMC3R, hMC4R and hMC5R. Rational design of modulator compounds that are analogous to endogenous melanocortins for these receptors presents a method to artificially regulate abnormalities.

While such endeavors have often been prefigured as the quintessential methodology for structure-based drug design in theory, the limited existing knowledge of the binding constructs of any given targeted membrane protein presents difficulties with novel drug discovery in practice[9]. The large size and irregular shape of membrane receptors (as well as most all soluble proteins) represent fairly formidable challenges in their successful crystallization for x-ray crystallographic analysis[10]. A general lack of the biophysical and three-dimensional structural information of membrane proteins renders the starting point of drug design as an iterative process of trial-and-error, integrating homology analyses, computational modeling, and ligand-binding studies in order to reconstruct the protein of interest. In particular, high-throughput screening (HTS) methods such as the classical

---

[1] Takeda, S. et al. *FEBS Letters* **2002**, *520*, 97.
[2] Tikhonova, I.G. et al. *Current Pharmaceutical Design* **2009**, *15*, 4003-016.
[3] Pierce, K. et al. *Nature Reviews Molecular Cell Biology* **2002**, *3*, 640.
[4] Lundstrom, K. *Methods in Molecular Biology* **2009**, *552*, 51.
[5] Cai, M. et al. *Current Topics in Medicinal Chemistry* **2009**, *9*, 554-555.
[6] Voisey, J. et al. *Current Drug Targets* **2003**, *4*, 593.
[7] Cone, R.D. *Nature Neuroscience* **2005**, *8*, 571.
[8] Voisey et al. *Current Drug Targets* **2003**, *4*, 586.
[9] Pierce, K. et al. *Nature Reviews Molecular Cell Biology* **2002**, *3*, 647.
[10] Dale, G.E. et al. *Journal of Structural Biology* **2003**, *142*, 92.

application of whole-cell, competitive radioligand binding and adenylate cyclase assays affords a relative evaluation of any library in terms of affinities and efficacies at certain membrane receptors *in vitro*. These combined methods represent the most practical means for probing the configuration of the extracellular loops forming the main binding sites on melanocortin receptors[11].

The focal point of this thesis is the high-throughput exploration of a library of *N*-methylated, multiple-disulfide cyclic peptides developed in Dr. David Craik's laboratory at the University of Queensland. These disulfide-rich peptides are based on the protein topology of conotoxins found in the venoms of marine cone snails. Because they are disulfide-rich, conotoxins are characterized by exceptional stability and a constrained, compact structure; they are also known to possess exquisite potency and selectivity[12]. Such properties make them and similar molecules (such as cyclotides) useful templates for novel drug design, especially in the treatment of pain[13]. Other activity-enhancing features of this class of compounds are their combined cyclic backbone and cystine knot motifs; these have been found to afford specific conformational constraining in addition to enhanced proteolytic stability and bioavailability[14]. As a supplementary study, the binding activity and therapeutic relevance of a series of linear molecular scaffolds from which this library was derived were was also assessed. These scaffolds represent modified versions of the naturally occurring peptides SFTI-1, odorranain-b1, and MCoTI-II, and lack the active pharmacophore of endogenous melanocyte stimulating hormone [His-Phe-Arg-Trp].

Also included is a discussion of the high-throughput exploration of a library of small molecule mimetics synthesized by Dr. James Cain, who was previously a graduate student in the Hruby group. Small molecules may be viewed as being complementary or even advantageous to peptide analogues with respect to applications in medicine, as dosages would presumably be lowered due to the decreased propensity for degradation by proteases[15]. With respect to synthesis, this library and similar compounds may be constructed from amino acids with relative ease compared to peptide synthesis[16].

Lastly, a discussion of the high-throughput assessment of a library of cyclized peptides produced by Dr. Joel Nyberg, who was previously a graduate student in the Hruby group, is also included. Backbone cyclization is a classical peptide ligand modification that decreases the degrees of freedom available to the molecule, thereby locking it into a limited number of conformational states; if the locked conformation is more favorable for binding than the linear state, cyclization can greatly increase the affinity and efficacy of a ligand[17]. Consequently, this also plays a role in ligand-receptor recognition and can enhance the selectivity and potency of a ligand for any given receptor subtype[18]. This library of compounds features the pharmacophore of the potent universal antagonist SHU-9119.

---

[11] Yeagle, P.L. et al. *Biochimica Et Biophysica Acta (BBA) – Biomembranes* **2007**, *1768*, 809-815.
[12] Clark, R.J. et al. *Proceedings of the National Academy of Sciences of the United States of America* **2005**, *102*, 13767.
[13] Clark, R.J. et al. *Proceedings of the National Academy of Sciences of the United States of America* **2005**, *102*, 13767.
[14] Daly, N.L. et al. *Advanced Drug Delivery Reviews* **2009**, *61*, 918.
[15] Cain, J.P. et al. *Bioorganic & Medicinal Chemistry Letters*, **2006**, 16, 5462-5467.
[16] Cain, J.P. et al. *Bioorganic & Medicinal Chemistry Letters*, **2006**, 16, 5462-5467.
[17] Fung, S. et al. Current Opinion in Chemical Biology **2005**, *9*, 352-358.
[18] Fung, S. et al. Current Opinion in Chemical Biology **2005**, *9*, 352-358.

Methods

Cell Culture

Human embryonic kidney clone 293 (HEK 293) cells stably transfected to overexpress each of hMC1R, hMC3R, hMC4R, C-terminal histidine-tagged hMC4R, and hMC5R were grown in whole minimum essential medium (MEM) containing by volume 10% fetal bovine serum (FBS), 1% sodium pyruvate, and 1% of a mixture of Penicillin and Streptomycin (Pen Strep) in plastic flasks. These cultures were maintained with G418, an antibiotic that blocks peptide synthesis in cells that do not express the target gene, at a working concentration of 0.5 mg/mL. After growing to confluence on the flask surface, the cells were washed briefly with phosphate buffered saline (PBS) before harvest or media change. If necessary, the cells were treated with a 0.25% saline solution of trypsin, a digestive enzyme that cleaves the proteins adhering the cells to the flask. They were then harvested by suspension in whole MEM for seeding 96-well assay plates, preparing petri dish cultures for protein purification, or seeding fresh flasks for the growth of new generations. Alternatively, suspension in cell-freezing medium containing DMSO enabled cryogenic storage of the cells.

Whole-cell Radioligand Binding Assay

The whole-cell competitive binding assay provides a relative assessment of the binding affinities of a library of analogues by permitting binding at melanocortin receptors in the presence of the nonselective radioligand, [^{125}I]-[Nle^{4}, D-Phe^{7}]α-MSH (NDP-α-MSH). The nonspecific, high-affinity agonist Ac-Nle-c[Asp-His-D-Phe-Arg-Trp-Lys]-NH_2 (Melanotan II, or MT-II) was used as a reference.

The aforenamed HEK 293 cells were grown to confluence and seeded in 96-well plates roughly 48 hours before the assay to ultimately yield approximately 50,000 cells per well. To prepare them for assaying, the cells were first aspirated of the growth media. A ten-fold serial dilution comprised of six concentrations of the analogue of interest (10^{-10} M to 10^{-5} M) in binding buffer was then added to the cells; all concentrations of the analogue were duplicated across two wells. 0.0125 μCi of the nonselective radioligand [^{125}I]-NDP-α-MSH were also added at this time. After incubating for 30 minutes at 37 °C, the cells were aspirated and lysed by the addition of 0.1 M NaOH and 1% Triton-X. Scintillation cocktail was added, and the radioactivity in counts per minute (CPM) of each well was measured by a Microbeta scintillation counter.

Analysis of Whole-cell Radioligand Binding Assay Results

Data from whole-cell binding assays were plotted and fitted as one-site competitive, six-point binding curves (CPM per well versus log[analogue]) using Graphpad Prism 5.0. The degree to which the known radioligand [^{125}I]-NDP-α-MSH was displaced by the nonspecific agonist MT-II determined maximal binding efficiency. The background CPM was determined by MT-II, and was subtracted from the data of the other analogues. The ratio of the bottom to top values of each analogue's binding curve multiplied by 100 and subtracted from 100 then gave the relative binding efficiency of that analogue compared to MT-II. Standard deviations were generated from the results of at least two assays.

Adenylate Cyclase Activity Assay

The functional secondary messenger assay provides a relative assessment (compared to the non-specific superpotent agonist MT-II) of the agonistic or antagonistic potency of a library of analogues by determination of the concentration of intracellular cAMP generated as a result of each analogue's binding at melanocortin receptors.

The aforenamed HEK 293 cells were grown to confluence and seeded in 96-well plates roughly 48 hours before the assay to ultimately yield approximately 50,000 cells per well. To prepare them for assaying, the cells were first aspirated of the growth media, washed with MEM, and incubated for 10 minutes at 37 °C with a 625 μM buffer of 3-isobutyl-1-methylxanthine (IBMX), a phosphodiesterase inhibitor that prevents the breakdown of intracellular cAMP. A ten-fold serial dilution comprised of six concentrations of the analogue of interest (10^{-10} M to 10^{-5} M) in MEM was then added to the cells; all concentrations of the analogue were duplicated across two wells. After incubating for 20 minutes at 37 °C, the cells were aspirated and lysed by the addition of an ice-cold lysis buffer of 20 mM tris-HCl, 30 mM tris-base, and 4 mM EDTA. The lysate was then was heat-shocked for 10 minutes in boiling water and frozen overnight at -20 °C.

The next day, the plates were thawed and centrifuged for 10 minutes at 4,000 RPM, and the cAMP-rich supernatant was transferred to fresh plates for the addition of 30 μCi of competitive [^{3}H]-cAMP in Tris-EDTA buffer and 60 μg/mL of protein kinase A (PKA) in Tris-EDTA buffer. These two solutions were also added to a standard of 11 concentrations of cAMP (32, 28, 24, 20, 16, 12, 8, 4, 2, 1, and 0 pmol/50 μL of Tris-EDTA buffer). To determine the background CPM, a blank containing only [^{3}H]-cAMP and neither cAMP nor PKA was also prepared at this time. The plates were incubated on ice for three hours, during which time competitive binding between [^{3}H]-cAMP and cAMP generated by the analogue took place at PKA.

The solution was then transferred to 96-well fiberglass filter allowing only the passage of particles smaller than a cAMP-PKA bound complex (1.0 μm). The CPM of each well after filtration was measured by a Microbeta scintillation counter following the addition of scintillation cocktail.

Analysis of Adenylate Cyclase Assay Results

Data from activity assays were plotted and fitted as six-point sigmoidal dose-response curves (pmol cAMP per well versus log[analogue]) using Graphpad Prism 5.0. The concentration of intracellular cAMP generated by the analogue was back-calculated from the radioactivity in CPM of each well determined by the Microbeta scintillation counter. The concentration of cAMP generated by the nonspecific, superpotent agonist MT-II defined maximal cellular response. The ratio of the top value of each analogue's dose-response curve to the top value of MT-II's curve multiplied by 100 then gave the relative percent of maximal response induced by that particular analogue. Standard deviations were generated from the results of at least two assays.

Results

For the following data analysis, low IC_{50} and EC_{50} values indicate high affinity and efficacy, respectively. Agonists are defined as compounds which exhibit high efficacy at a receptor; they induce secondary messenger activity. Antagonists are defined as compounds which repress secondary messenger activity. Whether a compound is classified as selective depends on how well it discriminates one receptor subtype, via affinity/efficacy, against the others. Standard deviations are reported for compounds which have been assayed two times, each assay containing duplicate assessments.

David Craik's Cyclic Knot Peptides

The affinities and efficacies of the Craik peptides at hMC1R, hMC3R, hMC4R, and hMC5R are presented in **Table 1a**. Several universal agonists and antagonists of the melanocortin receptors were identified from the library with mid- to high-nanomolar IC_{50} values; however, the binding affinities of each compound at the different receptor subtypes were often slightly dissimilar. Universal agonists included PC13a, PC13b, PC4, and PC12a, the latter three of which exhibit higher affinity for hMC1R, as indicated by their lesser EC_{50} and IC_{50} values. The universal antagonists were identified to be PC1 (with noted potency and affinity for hMC3R), PC22a, PC24a, and PC29.

In addition to the nonselective compounds, selective agonists and antagonists were also identified from this library. PC2, PC3, and PC24b were identified as hMC1R-selective agonists. PC19c was identified as an hMC1R-selective antagonist with exceptional affinity for hMC4R and hMC5R.

PC20a was identified as an hMC3R-selective agonist.

PC11a, PC11b, and PC19b were identified as partial selective antagonists of hMC4R, and PC30 was identified as a selective full antagonist of hMC4R. PC30 was also observed to exhibit affinity for hMC5R, at which it acted agonistically.

Lastly, several hMC5R-selective compounds were identified. PC16b and PC18a exhibited selective antagonism of hMC5R; however, partial antagonism of hMC4R by PC18a was also observed.

Supplementary Analysis of David Craik's Cyclic Knot Peptide Scaffolds

The affinities of molecular scaffolds derived from SFTI-1 at hMC1R, hMC3R, hMC4R, and hMC5R are presented in **Table 1b**. The binding efficiency of the scaffold models was generally limited to less than 50%; in many cases, no binding was observed whatsoever. Exceptions included MM7, MM8, MM9, and MM14, which were exhibited moderate to exceptional binding with low micromolar IC_{50} values.

James Cain's Small Molecules

The affinities and efficacies of the small molecule mimetics are presented in **Table 2**. JPC 5140 was identified as a selective partial antagonist of hMC1R; its IC_{50} is at least two orders of magnitude

lesser at that target than at any other receptor. JPC 6007 was observed to be a selective, allosteric inhibitor of hMC3R; again, its IC_{50} is approximately two orders of magnitude lesser at this receptor relative to the others. JPC 8029, JPC 8042, and JPC 9034 appear to be selective allosteric inhibitors of hMC5R; the IC_{50} values of JPC 8029 and JPC 8042 are at least two orders of magnitude lesser at this target in comparison to the others, while the IC_{50} value of JPC 9034 is approximately one order of magnitude lesser.

Joel Nyberg's Cyclic Peptides

The affinities and efficacies of the cyclized peptides are presented in **Table 3**. All of the peptide analogues exhibited exceptional binding affinities for hMC1R and hMC4R, at which they acted agonistically. In contradistinction, all of the analogues exhibited moderate to exceptional binding at hMC3R and hMC5R, at which they acted antagonistically. No compound which was selective for a single receptor subtype was identified.

Name	Sequence	1R				3R			
		EC_{50} (nM)	%max	IC_{50} (nM)	%BE	EC_{50} (nM)	%max	IC_{50} (nM)	%BE
PC1	cyclo[G-R-C-T-**H-F-R-W**-P-I-C-F-P-D]	2800	13	720 ± 580	40	200	6	9.3	41
PC2	cyclo[**W**-R-C-T-A-S-I-P-P-I-C-**H-F-R**]	710	81	2100	80	/	10	13	24
PC3	cyclo[G-R-C-T-**H-d-Phe-R-W**-P-I-C-F-P-D]	2600	93	3000	56	/	20	14	22
PC4	cyclo[**W**-R-C-T-A-S-I-P-P-I-C-**H-d-Phe-R**]	81 ± 39	77	140 ± 120	89	1100 ± 650	77	1000 ± 680	66
PC11a	cyclo[**W**-R-C-T-A-S-I-P-P-I-C-**NMe-H-d-Phe-R**]	180	83	1400	94	5200	100	67	37
PC11b	cyclo[**W**-R-C-T-A-S-I-P-P-I-C-**NMe-H-d-Phe-R**]	540	100	1700	98	6600	100	86	51
PC12a	cyclo[**W**-R-C-T-A-S-I-P-P-I-C-**H-d-Phe-NMe-R**]	150 ± 39	85	60 ± 8.4	96	540 ± 190	80	1300 ± 87	83
PC12b	cyclo[**W**-R-C-T-A-S-I-P-P-I-C-**H-d-Phe-NMe-R**]	1200	100	99	100	5900	100	2400	96
PC13a	cyclo[**NMe-W**-R-C-T-A-S-I-P-P-I-C-**H-d-Phe-R**]	800 ± 910	92	360 ± 42	100	940 ± 150	92	2500 ± 530	90
PC13b	cyclo[**NMe-W**-R-C-T-A-S-I-P-P-I-C-**H-d-Phe-R**]	110 ± 110	84	280 ± 88	96	1000 ± 720	100	2000	92
PC14a	cyclo[**NMe-W**-R-C-T-A-S-I-P-P-I-C-**H-d-Phe-NMe-R**]	47	81	49	100	920	73	4600	100
PC14b	cyclo[**NMe-W**-R-C-T-A-S-I-P-P-I-C-**H-d-Phe-NMe-R**]	39 ± 25	80	70 ± 6.2	97	9200	93	5100 ± 3200	89
PC14c	cyclo[**NMe-W**-R-C-T-A-S-I-P-P-I-C-**H-d-Phe-NMe-R**]	120 ± 42	86	87 ± 7.0	100	NA	NA	NB	NB
PC15	cyclo[**NMe-W**-R-C-T-A-S-I-P-P-I-C-**NMe-H-d-Phe-R**]	450	64	1600	100	6100	100	NB	NB
PC16a	cyclo[**W**-R-C-T-A-S-I-P-P-I-C-**NMe-H-d-Phe-NMe-R**]	720 ± 500	90	780 ± 80	97	NA	NA	2600	52
PC16b	cyclo[**W**-R-C-T-A-S-I-P-P-I-C-**NMe-H-d-Phe-NMe-R**]	1100 ± 1300	94	580 ± 100	94	4800	100	4200 ± 1800	56
PC17a	cyclo[**NMe-W**-R-C-T-A-S-I-P-P-I-C-**NMe-H-d-Phe-NMe-R**]	260 ± 210	89	340 ± 59	97	NA	NA	NB	NB
PC17b	cyclo[**NMe-W**-R-C-T-A-S-I-P-P-I-C-**NMe-H-d-Phe-NMe-R**]	1300 ± 1700	88	190 ± 91	93	NA	NA	1300	59
PC18a	cyclo[G-R-C-T-**H-d-Phe-R-NMe-W**-P-I-C-F-P-D]	1800	78	1400	86	6800	100	1600	33
PC18b	cyclo[G-R-C-T-**H-d-Phe-R-NMe-W**-P-I-C-F-P-D]	1600	100	1300	97	3600	100	NB	NB
PC18c	cyclo[G-R-C-T-**H-d-Phe-R-NMe-W**-P-I-C-F-P-D]	3100	99	1600	89	960	100	NB	NB
PC19a	cyclo[G-R-C-T-**H-d-Phe-NMe-R-W**-P-I-C-F-P-D]	5200	100	4200	98	800	100	2200	93
PC19b	cyclo[G-R-C-T-**H-d-Phe-NMe-R-W**-P-I-C-F-P-D]	200	48	1500	100	2200	96	960	87
PC19c	cyclo[G-R-C-T-**H-d-Phe-NMe-R-W**-P-I-C-F-P-D]	1200	23	1600	100	850	71	2400	90
PC20a	cyclo[G-R-C-T-**NMe-H-d-Phe-R-W**-P-I-C-F-P-D]	77	12	2100	50	/	>50	3500	51
PC20b	cyclo[G-R-C-T-**NMe-H-d-Phe-R-W**-P-I-C-F-P-D]	7900	62	3.9	17	NA	NA	1900 ± 520	47
PC20c	cyclo[G-R-C-T-**NMe-H-d-Phe-R-W**-P-I-C-F-P-D]	NA	NA	2600	49	NA	NA	1700	39
PC21a	cyclo[G-R-C-T-**H-d-Phe-NMe-R-NMe-W**-P-I-C-F-P-D]	1700	53	830	92	/	>50	660	37
PC21b	cyclo[G-R-C-T-**H-d-Phe-NMe-R-NMe-W**-P-I-C-F-P-D]	2700	58	330	90	NA	NA	NB	NB
PC22a	cyclo[G-R-C-T-**NMe-H-d-Phe-R-NMe-W**-P-I-C-F-P-D]	NA	NA	NB	NB	NA	NA	770 ± 950	34
PC22b	cyclo[G-R-C-T-**NMe-H-d-Phe-R-NMe-W**-P-I-C-F-P-D]	0.50	12	NB	NB	/	>30	NB	NB
PC22c	cyclo[G-R-C-T-**NMe-H-d-Phe-R-NMe-W**-P-I-C-F-P-D]	NA	NA	NB	NB	/	>30	660	30
PC23	cyclo[G-R-C-T-**NMe-H-d-Phe-NMe-R-W**-P-I-C-F-P-D]	20	9	NB	NB	4300	100	7.0	19
PC24a	cyclo[G-R-C-T-**NMe-H-d-Phe-NMe-R-NMe-W**-P-I-C-F-P-D]	NA	NA	4900	85	NA	NA	250	20
PC24b	cyclo[G-R-C-T-**NMe-H-d-Phe-NMe-R-NMe-W**-P-I-C-F-P-D]	5800	70	7900	100	/	>20	NB	NB
SFTI-1	cyclo[G-R-C-T-K-S-I-P-P-I-C-F-P-D]	5	13	490 ± 690	39	NA	NA	21 ± 28	25
PC29	cyclo[**F-R-W**-V-C-G-E-T-C-V-G-G-T-C-N-T-P-G-C-T-C-S-W-P-V-C-T-R-**H**]	NA	NA	1700	28	NA	NA	NB	NB
PC30	cyclo[**d-Phe-R-W**-V-C-G-E-T-C-V-G-G-T-C-N-T-P-G-C-T-C-S-W-P-V-C-T-R-**F**	2700 ± 690	96	4800	92	7200	100	1700 ± 2300	40
Kalata B1	cyclo[G-L-P-V-C-G-E-T-C-V-G-G-T-C-N-T-P-G-C-T-C-S-W-P-V-C-T-R-N]	1.5 ± 1.9	13	550 ± 700	28	NA	NA	7000 ± 9900	52
MT-II	Ac-Nle-c[Asp-**His-D-Phe-Arg-Trp**-Lys]-NH_2	330 ± 400	100	29 ± 0.18	100	37 ± 1.2	100	54 ± 28	100

Table 1a. Efficacies and affinities of multiple-disulfide, cyclized MSH analogues at hMC1R, hMC3R, hMC4R, and hMC5R. Pharmacophore sequence is indicated in boldface. (NB indicates IC50 > 10,000 nM producing no significant binding; NA indicates EC50 > 10,000 nM producing no significant activity; / indicates data not yet determined.)

Name	Sequence	4R				5R			
		EC_{50} (nM)	%max	IC_{50} (nM)	%BE	EC_{50} (nM)	%max	IC_{50} (nM)	%BE
PC1	cyclo[G-R-C-T-**H-F-R-W**-P-I-C-F-P-D]	NA	NA	690	51	NA	NA	1800 ± 1800	52
PC2	cyclo[**W**-R-C-T-A-S-I-P-P-I-C-**H-F-R**]	NA	NA	2700	83	/	<20	210	61
PC3	cyclo[G-R-C-T-**H-d-Phe-R-W**-P-I-C-F-P-D]	2200	20	120	59	NA	NA	260	60
PC4	cyclo[**W**-R-C-T-A-S-I-P-P-I-C-**H-d-Phe-R**]	2600 ± 1900	68	320	59	2500 ± 2000	70	710 ± 630	78
PC11a	cyclo[**W**-R-C-T-A-S-I-P-P-I-C-**NMe-H-d-Phe-R**]	490	24	110	61	/	~100	1200	99
PC11b	cyclo[**W**-R-C-T-A-S-I-P-P-I-C-**NMe-H-d-Phe-R**]	1500	48	390	60	5400	100	1400	100
PC12a	cyclo[**W**-R-C-T-A-S-I-P-P-I-C-**H-d-Phe-NMe-R**]	480 ± 420	69	1800 ± 1600	77	1500	100	880 ± 680	83
PC12b	cyclo[**W**-R-C-T-A-S-I-P-P-I-C-**H-d-Phe-NMe-R**]	1500	100	910	50	1900	52	NB	NB
PC13a	cyclo[**NMe-W**-R-C-T-A-S-I-P-P-I-C-**H-d-Phe-R**]	600 ± 400	100	1000 ± 1500	73	2300 ± 260	61	970 ± 310	86
PC13b	cyclo[**NMe-W**-R-C-T-A-S-I-P-P-I-C-**H-d-Phe-R**]	420 ± 370	86	660 ± 590	77	3300 ± 4400	62	5100 ± 4600	93
PC14a	cyclo[**NMe-W**-R-C-T-A-S-I-P-P-I-C-**H-d-Phe-NMe-R**]	610	100	NB	NB	2500	70	NB	NB
PC14b	cyclo[**NMe-W**-R-C-T-A-S-I-P-P-I-C-**H-d-Phe-NMe-R**]	280 ± 23	59	2100 ± 3000	69	2200 ± 800	40	NB	NB
PC14c	cyclo[**NMe-W**-R-C-T-A-S-I-P-P-I-C-**H-d-Phe-NMe-R**]	2600 ± 2500	66	2900 ± 3500	81	NA	NA	1200 ± 490	96
PC15	cyclo[**NMe-W**-R-C-T-A-S-I-P-P-I-C-**NMe-H-d-Phe-R**]	990	62	1800	37	2100	94	NB	NB
PC16a	cyclo[**W**-R-C-T-A-S-I-P-P-I-C-**NMe-H-d-Phe-NMe-R**]	3100	100	560 ± 790	31	NA	NA	220	44
PC16b	cyclo[**W**-R-C-T-A-S-I-P-P-I-C-**NMe-H-d-Phe-NMe-R**]	700	71	22	54	NA	NA	6500 ± 8500	77
PC17a	cyclo[**NMe-W**-R-C-T-A-S-I-P-P-I-C-**NMe-H-d-Phe-NMe-R**]	2900 ± 630	55	30	53	NA	NA	6900 ± 8900	92
PC17b	cyclo[**NMe-W**-R-C-T-A-S-I-P-P-I-C-**NMe-H-d-Phe-NMe-R**]	NA	NA	3.2	45	NA	NA	NB	NB
PC18a	cyclo[G-R-C-T-**H-d-Phe-R-NMe-W**-P-I-C-F-P-D]	37	31	77	23	36	9	570	75
PC18b	cyclo[G-R-C-T-**H-d-Phe-R-NMe-W**-P-I-C-F-P-D]	580	52	NB	NB	/	<90	NB	NB
PC18c	cyclo[G-R-C-T-**H-d-Phe-R-NMe-W**-P-I-C-F-P-D]	0.41	14	/	/	/	~100	340	68
PC19a	cyclo[G-R-C-T-**H-d-Phe-NMe-R-W**-P-I-C-F-P-D]	9700	100	1700	96	/	~100	1500	100
PC19b	cyclo[G-R-C-T-**H-d-Phe-NMe-R-W**-P-I-C-F-P-D]	660	30	7.3	79	/	~100	150	54
PC19c	cyclo[G-R-C-T-**H-d-Phe-NMe-R-W**-P-I-C-F-P-D]	2200	50	1.8	70	480	96	190	61
PC20a	cyclo[G-R-C-T-**NMe-H-d-Phe-R-W**-P-I-C-F-P-D]	/	<10	15	35	NA	NA	280	58
PC20b	cyclo[G-R-C-T-**NMe-H-d-Phe-R-W**-P-I-C-F-P-D]	5800	48	310	52	8600	57	2600 ± 1400	68
PC20c	cyclo[G-R-C-T-**NMe-H-d-Phe-R-W**-P-I-C-F-P-D]	/	100	320	70	1500	27	NB	NB
PC21a	cyclo[G-R-C-T-**H-d-Phe-NMe-R-NMe-W**-P-I-C-F-P-D]	190	57	2.7	51	NA	NA	3700	100
PC21b	cyclo[G-R-C-T-**H-d-Phe-NMe-R-NMe-W**-P-I-C-F-P-D]	1200	88	53	52	7400	100	280	30
PC22a	cyclo[G-R-C-T-**NMe-H-d-Phe-R-NMe-W**-P-I-C-F-P-D]	890 ± 1100	12	1600 ± 2200	43	NA	NA	NB	NB
PC22b	cyclo[G-R-C-T-**NMe-H-d-Phe-R-NMe-W**-P-I-C-F-P-D]	210	29	34	34	NA	NA	940	71
PC22c	cyclo[G-R-C-T-**NMe-H-d-Phe-R-NMe-W**-P-I-C-F-P-D]	1900	41	8000	42	/	>50	1100	84
PC23	cyclo[G-R-C-T-**NMe-H-d-Phe-NMe-R-W**-P-I-C-F-P-D]	1.6	13	/	/	2800	56	280	41
PC24a	cyclo[G-R-C-T-**NMe-H-d-Phe-NMe-R-NMe-W**-P-I-C-F-P-D]	3300	23	970	63	1500	18	520	41
PC24b	cyclo[G-R-C-T-**NMe-H-d-Phe-NMe-R-NMe-W**-P-I-C-F-P-D]	NA	NA	/	/	NA	NA	NB	NB
SFTI-1	cyclo[G-R-C-T-K-S-I-P-P-I-C-F-P-D]	NA	NA	5600 ± 8000	69	NA	NA	240 ± 340	26
PC29	cyclo[**F-R-W**-V-C-G-E-T-C-V-G-G-T-C-N-T-P-G-C-T-C-S-W-P-V-C-T-R-**H**]	NA	NA	/	/	25	7	NB	NB
PC30	cyclo[**d-Phe-R-W**-V-C-G-E-T-C-V-G-G-T-C-N-T-P-G-C-T-C-S-W-P-V-C-T-R-**F**	NA	NA	2300 ± 3000	64	3300	100	200	43
Kalata B1	cyclo[G-I-P-V-C-G-E-T-C-V-G-G-T-C-N-T-P-G-C-T-C-S-W-P-V-C-T-R-N]	NA	NA	0.21	51	NA	NA	2000 ± 1900	64
MT-II	Ac-Nle-c[Asp-**His-D-Phe-Arg-Trp**-Lys]-NH_2	200 ± 270	100	18 ± 25	100	170 ± 160	100	160 ± 150	100

Table 1a (continued). Efficacies and affinities of multiple-disulfide, cyclized MSH analogues at hMC1R, hMC3R, hMC4R, and hMC5R. Pharmacophore sequence is indicated in boldface. (NB indicates IC50 > 10,000 nM producing no significant binding; NA indicates EC50 > 10,000 nM producing no significant activity; / indicates data not yet determined.)

Name	Sequence	1R				3R			
		EC_{50} (nM)	%max	IC_{50} (nM)	%BE	EC_{50} (nM)	%max	IC_{50} (nM)	%BE
MM1	A-A-L-K-G-C-W-T-K-S-I-P-P-K-P-C-F-G-K-R	/	/	NB	NB	/	/	170	32
MM2	L-K-G-C-W-T-K-S-I-P-P-K-P-C-F-G-K	/	/	NB	NB	/	/	0.55	20
MM3	S-A-P-R-G-C-W-T-K-S-Y-P-P-K-P-C-K-amide—	/	/	1.9	8	/	/	NB	NB
MM4	Y-L-K-G-C-W-T-K-S-Y-P-P-K-P-C-F-S-R-amide—	/	/	NB	NB	/	/	NB	NB
MM5	S-V-I-G-C-W-T-K-S-I-P-P-R-P-C-F-V-K-amide—	/	/	NB	NB	/	/	NB	NB
MM6	C-Y-I-Q-N-C-P-R-G-G-K-amide	/	/	0.048	30	/	/	NB	NB
MM7	G-A-L-R-G-C-W-T-K-S-Y-P-P-K-P-C-K-amide—	/	/	NB	NB	/	/	8.6	4
MM8	A-A-L-K-G-C-W-T-K-S-I-P-T-K-P-C-F-G-K-R	/	/	2.2	17	/	/	NB	NB
MM9	L-K-G-C-W-T-K-S-I-P-T-K-P-C-F-G-K	/	/	280	29	/	/	NB	NB
MM10	G-G-V-C-P-K-I-L-K-K-C-R-R-D-S-D-C-P-G-A-C-I-C-R-G-N-G-Y-C-G-S-G-S-D	/	/	5.0	15	/	/	9.9	16
MM11	G-A-C-T-K-S-I-P-P-I-C-F-P-D	/	/	11	19	/	/	NB	NB
MM12	G-R-C-T-A-S-I-P-P-I-C-F-P-D	/	/	NB	NB	/	/	NB	NB
MM13	G-R-C-T-K-S-A-P-P-I-C-F-P-D	/	/	1.5	25	/	/	0.12	14
MM14	G-R-C-T-K-S-I-P-A-I-C-F-P-D	/	/	1.0	26	/	/	1400	56
MM15	G-R-C-T-K-S-I-P-P-I-C-A-P-D	/	/	7600	27	/	/	NB	NB
MM16	G-R-C-T-K-S-I-P-P-R-C-F-P-D	/	/	NB	NB	/	/	NB	NB
MT-II	Ac-Nle-c[Asp-**His-D-Phe-Arg-Trp**-Lys]-NH_2	/	/	20	100	/	/	44	100

Table 1b. Affinities of disulfide-rich, linear molecular scaffolds at hMC1R, hMC3R, hMC4R, and hMC5R.
(NB indicates IC50 > 10,000 nM producing no significant binding; NA indicates EC50 > 10,000 nM producing no significant activity; / indicates data not yet determined.)

Name	Sequence	4R				5R			
		EC_{50} (nM)	%max	IC_{50} (nM)	%BE	EC_{50} (nM)	%max	IC_{50} (nM)	%BE
MM1	A-A-L-K-G-C-W-T-K-S-I-P-P-K-P-C-F-G-K-R	/	/	NB	NB	/	/	0.51	33
MM2	L-K-G-C-W-T-K-S-I-P-P-K-P-C-F-G-K	/	/	NB	NB	/	/	0.40	45
MM3	S-A-P-R-G-C-W-T-K-S-Y-P-P-K-P-C-K-amide—	/	/	NB	NB	/	/	1100	33
MM4	Y-L-K-G-C-W-T-K-S-Y-P-P-K-P-C-F-S-R-amide—	/	/	NB	NB	/	/	12	29
MM5	S-V-I-G-C-W-T-K-S-I-P-P-R-P-C-F-V-K-amide—	/	/	NB	NB	/	/	1.7	20
MM6	C-Y-I-Q-N-C-P-R-G-G-K-amide	/	/	NB	NB	/	/	160	33
MM7	G-A-L-R-G-C-W-T-K-S-Y-P-P-K-P-C-K-amide—	/	/	NB	NB	/	/	1600	57
MM8	A-A-L-K-G-C-W-T-K-S-I-P-T-K-P-C-F-G-K-R	/	/	8900	100	/	/	8.3	39
MM9	L-K-G-C-W-T-K-S-I-P-T-K-P-C-F-G-K	/	/	7000	100	/	/	0.16	24
MM10	G-G-V-C-P-K-I-L-K-K-C-R-R-D-S-D-C-P-G-A-C-I-C-R-G-N-G-Y-C-G-S-G-S-D	/	/	NB	NB	/	/	/	/
MM11	G-A-C-T-K-S-I-P-P-I-C-F-P-D	/	/	NB	NB	/	/	NB	NB
MM12	G-R-C-T-A-S-I-P-P-I-C-F-P-D	/	/	5.3	31	/	/	200	15
MM13	G-R-C-T-K-S-A-P-P-I-C-F-P-D	/	/	NB	NB	/	/	140	16
MM14	G-R-C-T-K-S-I-P-A-I-C-F-P-D	/	/	2100	72	/	/	NB	NB
MM15	G-R-C-T-K-S-I-P-P-I-C-A-P-D	/	/	NB	NB	/	/	2.7	5
MM16	G-R-C-T-K-S-I-P-P-R-C-F-P-D	/	/	NB	NB	/	/	NB	NB
MT-II	Ac-Nle-c[Asp-**His-D-Phe-Arg-Trp**-Lys]-NH_2	/	/	540	100	/	/	340	100

Table 1b (continued). Affinities of disulfide-rich, linear molecular scaffolds at hMC1R, hMC3R, hMC4R, and hMC5R.
(NB indicates IC50 > 10,000 nM producing no significant binding; NA indicates EC50 > 10,000 nM producing no significant activity; / indicates data not yet determined.)

Results

Name	Structure/Sequence	1R				3R			
		EC_{50} (nM)	%max	IC_{50} (nM)	BE	EC_{50} (nM)	%max	IC_{50} (nM)	BE
JPC 5140	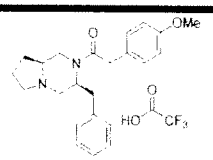	550 ± 770	19	45 ± 45	49	NA	0	5800	100
JPC 5151	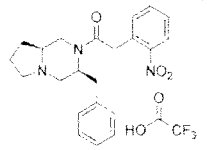	NA	0	450 ± 640	76	NA	0	ND	ND
JPC 6007	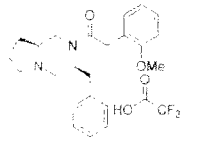	NA	0	3300 ± 4600	100	NA	0	26	46
JPC 6072	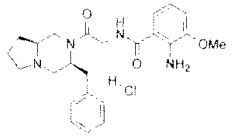	NA	0	1000 ± 1500	88	NA	0	4000	100
JPC 8029	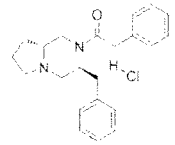	NA	0	3200 ± 4500	ND	NA	0	2500	100
JPC 8042	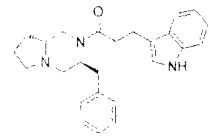	NA	0	3400 ± 4800	100	NA	0	3800	100
JPC 9011	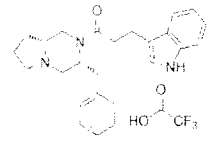	NA	0	7000 ± 9900	39	2700 ± 390	51	ND	ND
JPC 9031	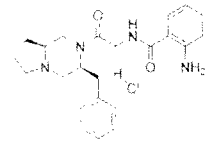	NA	0	1200 ± 1700	80	NA	0	1100	88
JPC 9034	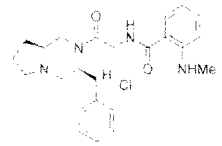	NA	0	1200 ± 1500	61	NA	0	270	33
MT-II	Ac-Nle-c[Asp-**His-D-Phe-Arg-Trp**-Lys]-NH2	24 ± 26	100	7.0 ± 3.8	100	140 ± 210	100	47 ± 37	100

Table 2. Efficacies and affinities of small molecule mimetics at hMC1R, hMC3R, hMC4R, and hMC5R.

(NB indicates IC50 > 10,000 nM producing no significant binding; NA indicates EC50 > 10,000 nM producing no significant activity.)

Results

Name	Structure/Sequence	4R				5R			
		EC_{50} (nM)	%max	IC_{50} (nM)	BE	EC_{50} (nM)	%max	IC_{50} (nM)	BE
JPC 5140	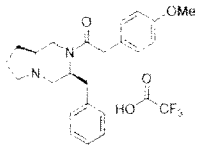	NA	0	NB	0	NA	0	5700	100
JPC 5151	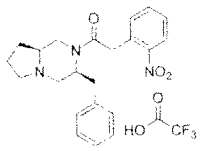	NA	0	NB	0	NA	0	0.54	64
JPC 6007	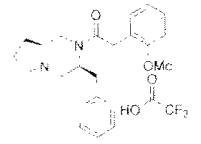	NA	0	NB	0	NA	0	1700	82
JPC 6072	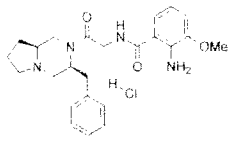	NA	0	NB	0	NA	0	1400	87
JPC 8029	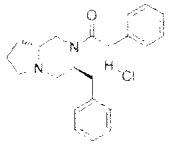	NA	0	NB	0	NA	0	7.6	56
JPC 8042	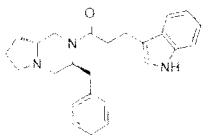	NA	0	NB	0	NA	0	0.74	62
JPC 9011	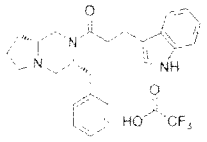	NA	0	NB	0	NA	0	1600	90
JPC 9031	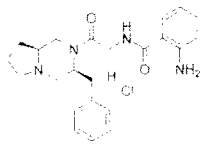	NA	0	NB	0	NA	0	140	72
JPC 9034	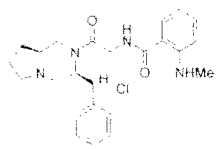	NA	0	480	100	90 ± 110	5	29 ± 36	85
MT-II	Ac-Nle-c[Asp-**His-D-Phe-Arg-Trp**-Lys]-NH2	46 ± 35	100	4.1	100	160 ± 170	100	9.3 ± 8.3	100

Table 2 (continued). Efficacies and affinities of small molecule mimetics at hMC1R, hMC3R, hMC4R, and hMC5R.

(NB indicates IC50 > 10,000 nM producing no significant binding; NA indicates EC50 > 10,000 nM producing no significant activity.)

Results

Name	Structure/Sequence	1R				3R			
		EC_{50} (nM)	%max	IC_{50} (nM)	BE	EC_{50} (nM)	%max	IC_{50} (nM)	BE
JBN 103	Ac-Nle-c[Asp-**His-DNal(2')-Arg-Trp**-Lys]-Gly-Lys-Pro-Val-NH2	150 ± 190	98	8.1 ± 2.5	96	490 ± 190	5	11 ± 8.1	100
JBN 105	Ac-Nle-c[Asp-**His-DNal(2')-Arg-Trp**-Lys]-Ala-Lys-Pro-Val-NH2	3300 ± 4600	100	7.8 ± 2.3	95	2600 ± 3100	13	16 ± 14	100
JBN 107	Ac-Nle-c[Asp-**His-DNal(2')-Arg-Trp**-Lys]-Ala-Gly-Lys-Pro-Val-NH2	40 ± 18	87	9.4 ± 1.7	94	NA	0	21 ± 26	100
JBN 109	Ac-Nle-c[Asp-**His-DNal(2')-Arg-DNal(2')**-Lys]-Ala-Gly-Lys-Pro-Val-NH2	41 ± 55	94	3.5 ± 1.6	98	NA	0	11 ± 11	99
JBN 111	Ac-Nle-c[Asp-**His-DNal(2')-Arg-DNal(2')**-Lys]-Gly-Lys-Pro-Val-NH2	18 ± 13	87	3.9 ± 0.060	96	170 ± 160	16	5.8 ± 5.0	97
JBN 113	Ac-Nle-c[Asp-**His-DNal(2')-Arg-DNal(2')**-Lys]-Ala-Lys-Pro-Val-NH2	21 ± 8.3	100	7.7 ± 3.5	99	NA	0	11 ± 12	99
MT-II	Ac-Nle-c[Asp-**His-D-Phe-Arg-Trp**-Lys]-NH2	24 ± 26	100	7.0 ± 3.8	100	140 ± 210	100	47 ± 37	100

Table 3. Efficacies and affinities of cyclized peptide analogues at hMC1R, hMC3R, hMC4R, and hMC5R. Pharmacophore sequence is indicated in boldface.
(NB indicates IC50 > 10,000 nM producing no significant binding; NA indicates EC50 > 10,000 nM producing no significant activity.)

Name	Structure/Sequence	4R				5R			
		EC_{50} (nM)	%max	IC_{50} (nM)	BE	EC_{50} (nM)	%max	IC_{50} (nM)	BE
JBN 103	Ac-Nle-c[Asp-**His-DNal(2')-Arg-Trp**-Lys]-Gly-Lys-Pro-Val-NH2	550 ± 600	80	610	100	NA	0	6.1 ± 6.0	97
JBN 105	Ac-Nle-c[Asp-**His-DNal(2')-Arg-Trp**-Lys]-Ala-Lys-Pro-Val-NH2	120 ± 130	73	130	82	1000 ± 850	10	5.4 ± 7.3	97
JBN 107	Ac-Nle-c[Asp-**His-DNal(2')-Arg-Trp**-Lys]-Ala-Gly-Lys-Pro-Val-NH2	170 ± 170	68	930	92	760 ± 910	23	7.6 ± 6.6	98
JBN 109	Ac-Nle-c[Asp-**His-DNal(2')-Arg-DNal(2')**-Lys]-Ala-Gly-Lys-Pro-Val-NH2	25 ± 3.3	42	590	74	NA	0	4.3 ± 3.9	98
JBN 111	Ac-Nle-c[Asp-**His-DNal(2')-Arg-DNal(2')**-Lys]-Gly-Lys-Pro-Val-NH2	54 ± 35	40	23	69	1300 ± 880	3	6.6 ± 6.0	96
JBN 113	Ac-Nle-c[Asp-**His-DNal(2')-Arg-DNal(2')**-Lys]-Ala-Lys-Pro-Val-NH2	38 ± 34	34	57	100	2300 ± 520	9	18 ± 8.0	98
MT-II	Ac-Nle-c[Asp-**His-D-Phe-Arg-Trp**-Lys]-NH2	46 ± 35	100	4.1	100	160 ± 170	100	9.3 ± 8.3	100

Table 3 (continued). Efficacies and affinities of cyclized peptide analogues at hMC1R, hMC3R, hMC4R, and hMC5R. Pharmacophore sequence is indicated in boldface. (NB indicates IC50 > 10,000 nM producing no significant binding; NA indicates EC50 > 10,000 nM producing no significant activity.)

Discussion

The approach of rational drug design on the basis of structure-activity relationships (SARs) entails careful consideration of the ligand-receptor interactions that govern the docking of the ligand in the binding pocket and the subsequent activation or inhibition of the receptor.

As previously mentioned, GPCRs possess a signature folding pattern which produces seven α-helical domains that span the lipid bilayer and are arranged in a largely universal fashion (**Figure 1**)[19]. Joining these together in series are three extracellular loops (EL1, 2, 3) and three intracellular loops (IL1, 2, 3) that fall on either side of the plasma membrane and represent the majority of variability from one GPCR to another. In addition, the extracellular N-terminus and the intracellular C-terminus are significant in signal recognition and intracellular protein binding. Accordingly, the diversity and specificity of GPCR activity may be ascribed to these variable regions, particularly that of the second extracellular loop (EL2), which plays a critical role in ligand binding[20].

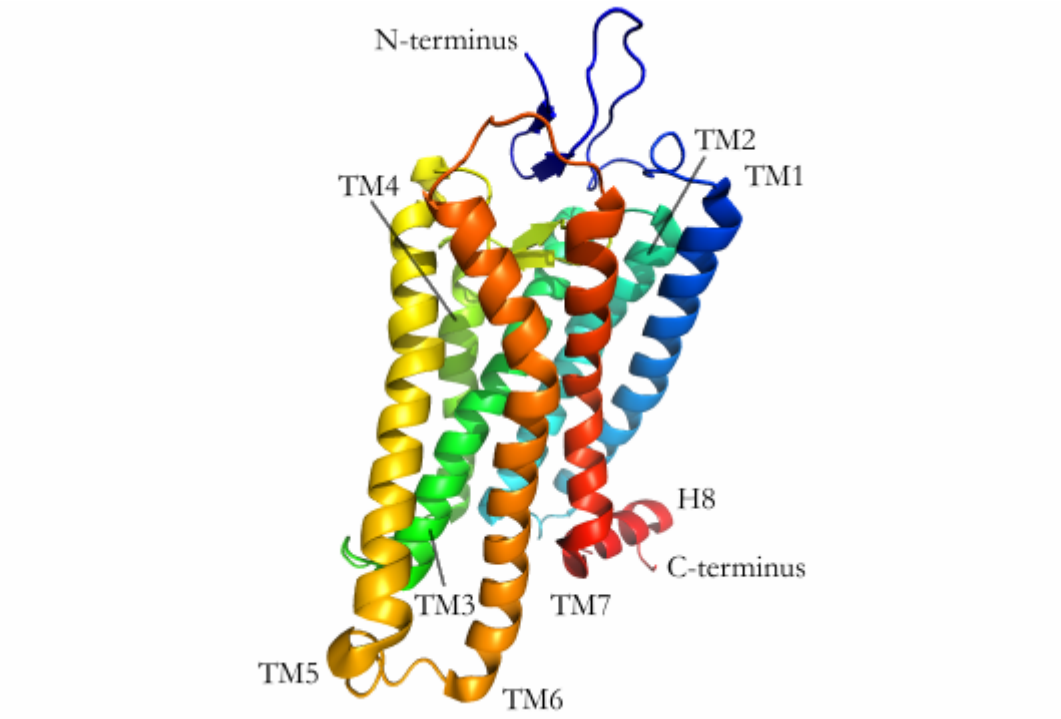

Figure 1. The crystal structure of bovine rhodopsin, a prototypical GPCR (Stenkamp, R.E. *Acta Crystallographica Section D Biological Crystallography* **2008**, *64*, 902-04.)

Binding with efficiency onto the biological surface of the target GPCR is a critical initial step to a ligand's ability to affect change in the activity of the target cell; this process is directed by the strength of the interactions between the functional groups on the interfaces of the ligand-receptor system[21]. In this respect, a successful ligand is one whose entropy of binding is offset by its corresponding release of enthalpy due to binding, largely attributable to formation of hydrogen

[19] Yeagle, P.L. et al. Biochimica Et Biophysica Acta (BBA) - Biomembranes **2007**, 1768, 808-24.
[20] Tikhonova, I.G. et al. *Current Pharmaceutical Design* **2009**, *15*, 4003-016.
[21] Erhardt, Paul. *Pharmacology: Principles and Practice*, **2009**, 475-560.

bonds and favorable hydrophobic interactions[22]. These interactions stabilize the ligand as it enters the binding pocket. Similarly, the ligand must also promote an electrostatically favorable spread of electronic density across the binding surfaces, and must be of an appropriate size, shape, and orientation so as to maximize the total number of stabilizing interactions across the interface. Finally, the ligand must possess the correct properties to modulate the target receptor as intended after successfully binding. For the purposes of the discussions in this thesis, affinity and efficacy of any given ligand will be addressed in terms of the IC_{50} and EC_{50} values respectively, wherein the IC_{50} represents the concentration of the ligand required to displace 50% of the specific binding of the competing radioligand, and the EC_{50} represents the concentration of the ligand required to induce 50% of the maximum secondary messenger activity.

With nearly 1000 different GPCRs encoded in the human genome, it is clear that the challenge of drug design is both an arduous and auspicious one (Pierce et al., 2002)[23]. Because the unique chemical parameters of the target GPCR surface determine the nature of its reciprocal ligand, GPCR-based drug discovery provides an opportunity to create ligands with remarkable selectivity; the identification of a hit in the laboratory may be followed by its systematic and iterative optimization, ultimately yielding an exceptionally effective ligand *in vitro*—and, potentially, a therapeutically relevant drug *in vivo*.

David Craik's Cyclic Knot Peptides

While bioactive peptides have long been utilized in targeting regulatory proteins for the treatment of disease in humans, they have not typically exhibited the cyclic, disulfide-rich frameworks which distinguish conotoxins and similar molecules as novel chemotherapeutic scaffolds for the development of treatment options for conditions associated with the central nervous system[24].

Cyclotides and conotoxins are naturally occurring toxins found in nature in terrestrial plants and the venoms of marine cone snails[25]. Both classes of peptides typically contain between 12 and 30 amino acids, making them slightly larger than traditional small molecule drugs, and both exhibit extensive disulfide bond connectivity[26]. Cyclotides in particular are known to exhibit a distinctive structural motif known as a cystine knot. The cystine knot is characterized by threading of a disulfide bond through a loop comprised of two other disulfide bonds and the segments of residues which connect them, and is known to impart considerable structural stability to the peptide[27].

In cyclotides, this interlocking disulfide topology is important both in defining the folding pattern of the peptide and its structural integrity, and occurs in conjunction with a cyclized backbone; combined, these two structural motifs are referred to as a cyclic cystine knot (CCK)[28]. The CCK framework also imparts additional stability by "locking" the peptide into a true knot, which cannot unfold unless a bond within the motif is broken. In reality, even peptides exhibiting two-disulfide bond versions of the CCK framework have been shown to adopt a native cyclotide fold, illustrating

[22] Patil, R. et al. *PLoS ONE* **2010**, *5*.
[23] Pierce, K.L. et al. *Nature Reviews Molecular Cell Biology* **2002**, *3*, 639-650.
[24] Clark, R.J. et al. *Proceedings of the National Academy of Sciences of the United States of America* **2005**, *102*, 13767.
[25] Craik, D.J. et al. *Chimica Oggi—Chemistry Today* **2005**, *26*, 20.
[26] Clark, R.J. et al. *Proceedings of the National Academy of Sciences of the United States of America* **2005**, *102*, 13767.
[27] Daly, N.L. et al. *Advanced Drug Delivery Reviews* **2009**, *61*, 923.
[28] Korsinczky M.L.J. et al. *Biochemistry* **2005**, *44*, 1151.

the degree of biological integrity this structure is capable of imparting[29]. These properties of cyclotides have made them an exciting prospect for the development of therapeutically stable treatment options.

A related class of molecules, conotoxins, has also received attention as useful scaffolds for drug discovery[30]. Conotoxins are similar to cyclotides in that they are also relatively small disulfide-rich compounds (possessing up to three disulfide bonds), but occur in nature as linear peptides rather than cyclized ones[31]. For this reason, they are, as with many peptide chemotherapeutics, rather susceptible to proteolysis if administered for use *in vivo*.

Both classes of compounds represent a lucrative aim for drug discovery due to their exceptional potency and selectivity as alternatives to other forms of treatment which may be met with tolerance over time, such as morphine and antidepressants[32]. In addition, natural conotoxin bioactivity occurs by a wide variety of mechanisms, including modulation and blockage of ion channels, transporter inhibition, and both non-competitive and competitive antagonism of receptors[33]. The array of molecular targets these compounds invoke implies that highly customizable treatment options may be developed for a diverse range of conditions. Conotoxins have been most notably relevant to the management of neuropathic pain and its associated conditions[34].

To increase the biostability of disulfide-rich analogues while retaining the neurophysiological benefits they may impart, cyclization may be performed. The analogues described in **Table 1a** are peptides of 14 or 29 residues, cyclized by native chemical ligation (NCL)[35]. In this reaction, a C-terminal thioester undergoes intramolecular nucleophilic attack by an N-terminal cysteine side chain; this results in the formation of a thioester-linked intermediate, which rearranges through a 5-membered ring to form the native amide bond[36]. This method allows for the formation of a native peptide bond at the ligation site. In addition to increasing the structural integrity of a peptide ligand, cyclization also confers resistance to disulfide scrambling and reduction, which may produce inactive derivatives[37]. It may also be used to increase affinity and potency at desired molecular targets by constraining pharmacophores to more active conformations[38].

The analogues in **Table 1a** also feature *N*-methylation, another classical ligand modification. The replacement of protons by methyl groups on amides of peptide bonds alters the biological properties of the analogue by transforming its lipophilicity, an important element in the determination of its pharmacokinetics and potential translocation across the plasma membranes of target cells[39]. It has also been shown to impart enhanced bioactivity to cyclic peptides such as vancomycin and cyclosporin A[40, 41]. Furthermore, multiple *N*-methylation of externally oriented

[29] Daly, N.L. et al. *Advanced Drug Delivery Reviews* **2009**, *61*, 923.
[30] Christopoulos, A. et al., *Biochemical Society Transactions* **2004**, *32*, 873.
[31] Clark, R.J. et al. *Proceedings of the National Academy of Sciences of the United States of America* **2005**, *102*, 13767.
[32] Clark, R.J. et al. *Angewandte Chemie-International Edition* **2010**, *49,* 6545.
[33] McIntosh, J.M. et al. *Toxicon* **2005**, *39*, 1449.
[34] Clark, R.J. et al. *Angewandte Chemie-International Edition* **2010**, *49,* 6545.
[35] Clark, R.J. et al., *Toxicon* **2012**, *59*, 446.
[36] Dawson, P.E. et al., *Science* **1994**, *266*, 776.
[37] Lovelace, E.S. et al. *Antioxidants and Redox Signaling* **2010**, *14*, 87-95.
[38] Daly, N.L. *European Biophysics Journal* **2011**, *40*, 367-368.
[39] Fairlie, D.P. et al. *Current Medicinal Chemistry* **1995**, *2*, 654-686.
[40] Smith, J.M. et al. *Journal of Clinical Pathology* **1983**, *36*, 41-43.
[41] Sangalli, L. et al. *Drug Metabolism and Disposition* **1988**, *16*, 749-753.

amide bonds on a cyclic peptide has been shown to produce a considerable improvement in the selectivity of a ligand for a specific receptor subtype[42,43]. Lastly, *N*-methylation enhances the proteolytic stability of many peptides by virtue of the steric shielding imparted by alkyl groups to the amide bonds on which they are substituted, thereby making these peptides less susceptible to endopeptidase activity[44].

Many of these compounds exhibited the pharmacophore sequence of MT-II, a superpotent, non-selective agonist of melanocortin receptors [His-D-Phe-Arg-Trp][45] in the context of cyclopeptide scaffolds based on the naturally occurring disulfide-rich cyclopeptides SFTI-1 and Kalata B1; others exhibited the pharmacophore of endogenous melanocyte stimulating hormone, [His-Phe-Arg-Trp]. These active core tetrapeptides systematically replaced four residues of the endogenous cyclopeptide scaffold, and were also systematically *N*-methylated in hopes of enhancing ligand selectivity. Lastly, each peptide was isolated in up to three conformational variants (notated by the lowercase letters following each compound's name).

The scaffold molecule into which the pharmacophore was inserted most extensively in this library was SFTI-1, a small, potent trypsin inhibitor which exhibits a circular backbone and compact rigidity due to three proline residues (**Figure 2**). At approximately one-half the size of the average cyclotide, SFTI-1 is comprised of 14 amino acids and possesses a single disulfide bond amidst an extensive hydrogen bond network[46]. The other scaffold molecule considered in this library was Kalata B1, a uterotonic cyclic peptide exhibiting a Möbius fold[47] and three disulfide bonds which form the cystine knot of the CCK motif; the cystine knot is characterized by threading of a disulfide bond through a loop comprised of two other disulfide bonds and the segments of residues which connect them[48] (**Figure 3**). Both scaffold molecules were observed to be universal antagonists of melanocortin receptors; these exhibited moderate binding efficiency at all the receptors and induced little or no cAMP activity.

The agonists identified from the library were analogues of SFTI-1 possessing the pharmacophore of MT-II; their universal activating quality suggests that implantation of the MT-II pharmacophore into a cyclic, single-disulfide framework results in retention of most of its bioactivity and by implication, its structure, to the degree that it actually reverses the naturally antagonistic property of SFTI-1 itself.

Among the universal antagonists identified, PC1 exhibited the endogenous, non-methylated MSH pharmacophore replacing four residues of the SFTI-1 scaffold. Because it brought about suppression of adenylate cyclase activity rather than activation, PC1 demonstrated—in addition to the previously described evidence that the pharmacophore activates the SFTI-1 scaffold—that it is also possible (depending on the site of insertion) that the pharmacophore's conformation may be altered and deactivated on incorporation. PC22a illustrated a similar outcome in the loss of agonistic quality when using a twice-methylated MT-II pharmacophore to replace four residues of the SFTI-1 scaffold; PC24a reproduces this effect with a triple-methylated pharmacophore. Interestingly, PC1, PC22a, and PC24a all exhibited pharmacophores incorporated at the same

[42] Chatterjee, J. et al. *Journal of Medicinal Chemistry* **2007**, *50*, 5878.
[43] Doedens, L. et al. *Journal of the American Chemical Society* **2010**, *132*, 8115.
[44] Cody, W.L. et al. *Journal of Medicinal Chemistry* **1997**, *40*, 2228-2240.
[45] Cai, M. et al. *Peptides* **2005**, *26*, 1482.
[46] Korsinczky M.L.J. et al. *Biochemistry* **2005**, *44*, 1151.
[47] Daly, N.L. et al. *Advanced Drug Delivery Reviews* **2009**, *61*, 919.
[48] Barbeta, B.L. et al. *PNAS*, **2008**, *105*, 1221.

position in the SFTI-1 scaffold. Again, this contradicts the above findings regarding the universal agonists of melanocortin receptors, suggesting that the site of replacement is critical to the modulation of the pharmacophore conformation, probably due to some change in secondary structure.

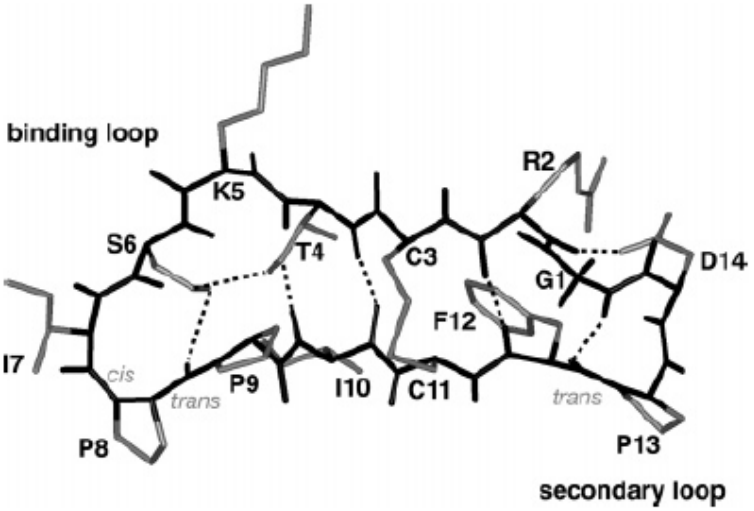

Figure 2. Structure of SFTI-1, a cyclic, potent trypsin inhibitor possessing a single disulfide bond supported by a hydrogen bond network. (Korsinczky, M.L.J. et al. *Biochemistry* **2005**, *44*, 1146.)

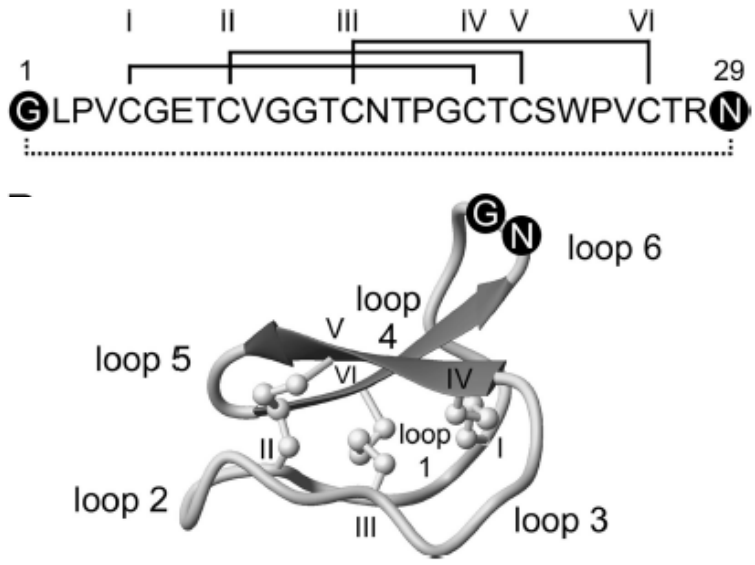

Figure 3. Structure and sequence with disulfide bond connectivities of Kalata B1, a uterotonic peptide exhibiting the cyclic cystine knot motif. (Barbeta, B.L. et al. *PNAS* **2008**, *105*, 1222.)

In addition to the nonselective compounds, selective agonists and antagonists were also identified from this library. The SFTI-1 analogues PC2, PC3, and PC24b were identified as hMC1R-selective agonists, exhibiting high binding efficiencies and efficacies at hMC1R relative to the other receptor subtypes; however, their EC_{50} and IC_{50} values generally remain in the high-nanomolar and low-

micromolar range, indicating that they are only of moderate potency. PC19c, also derived from SFTI-1, was identified as an hMC1R-selective antagonist exhibiting exceptional low- to mid-nanomolar affinity for hMC4R and hMC5R.

Only one hMC3R-selective compound was identified. The SFTI-1 analogue PC20a appears to activate hMC3R while repressing the other receptor subtypes; however, this conclusion has been drawn on the basis of percent maximal activity induced.

Several hMC4R-selective compounds were observed. The SFTI-1 analogues PC11a, PC11b, and PC19b exhibited exceptional affinity for hMC4R with IC_{50} values in the low- to mid-nanomolar range and produced partial selective antagonism of hMC4R. PC30 exhibited the implantation of the MT-II pharmacophore within the Kalata B1 scaffold, and was identified as a selective antagonist of hMC4R; however, its affinity for hMC5R (which it maximally upregulates) is high relative to that for the other receptor subtypes wherein it possesses mediocre IC_{50} values in the micromolar range. Thus, PC30 may also be interpreted as a semi-selective agonist of hMC5R.

Lastly, several hMC5R-selective compounds were identified. The SFTI-1 analogues PC16b and PC18a exhibited selective antagonism of hMC5R; however, partial antagonism of hMC4R by PC18a was also observed.

These screening results provide important starting points for the optimization of novel cyclic knot peptides targeting the melanocortin system.

Supplementary Analysis of David Craik's Cyclic Knot Peptide Scaffolds

As a complementary study, a series of molecular scaffolds on which the previously assessed library was loosely based was furnished by the Craik laboratory for assaying. These scaffolds are presented in **Table 1b** and represent modified versions of the naturally occurring cyclotides SFTI-1, odorranain-b1, and MCoTI-II.

From SFTI-1, the derivative scaffolds MM11 through MM16 were produced via linearization followed by the single replacement of one residue in the naturally occurring peptide. Residues 2, 5, 7, 9, and 12 were substituted one at a time by alanine to yield MM11 through MM15, and residue 10 was substituted by arginine to yield MM16. In all cases, the cysteine bridge characteristic of SFTI-1 was conserved.

Other compounds which were not used as explicitly as SFTI-1 to generate the previously assessed library were also included in this series of molecular scaffolds. Odorranain-b1, an antimicrobial protein recently isolated from the skin secretions of odorous frogs endemic to China, was included in both its naturally occurring sequence as MM1, as well as various modified forms as MM2 through MM5 and MM7 through MM9. Odorranain-b1 is a linear peptide comprised of 20 amino acids forming a random coil, a departure from the extended strand structure of SFTI-1[49]. However, odorranain-b1 is of similar size as SFTI-1, and both peptides possess a single cysteine bridge (though this disulfide bridge is observed to involve several more residues in odorranain-b1 than

[49] Wang, H. et al. *Peptides* **2012**, *35*, 285-290.

SFTI-1)[50]. Again, modification of this molecular scaffold afforded conservation of the cysteine bridge, and involved substitutions of amino acid residues throughout the coil, as well as varying truncations of the first and last several residues.

Another compound that influenced the previously assessed library was MCoTI-II, which was included in this series of molecular scaffolds in its naturally occurring sequence as MM10. MCoTI-II is a trypsin protease inhibitor that is more comparable to Kalata B1 in size at 34 amino acids; in addition, it possesses three cysteine bridges and a cyclic backbone as it is found in nature, and consequently exhibits the cyclic cystine knot structural motif characteristic of many larger cyclotides[51]. However, for the purposes of this assay, the peptide was linearized while conserving the three disulfide bonds.

Assays on these scaffold molecules were intended to serve as control experiments for the previously presented cyclic knot analogue library; while some of the scaffolds may have seemed closely related to the disulfide-rich analogues in size, sequence, and topology, the two groups of small proteins diverged in several critical ways. Firstly, the scaffold models exhibited linear rather than cyclized backbones; this change is expected to have a diminishing effect on the relative affinity and potency, as no additional conformational constraints apart from the cysteine bridges were incorporated[52]. Secondly and more critically, the scaffolds lacked the pharmacophore of endogenous melanocyte stimulating hormone, [His-Phe-Arg-Trp]. In essence, they lacked the key mechanism required to activate or even efficiently bind melanocortin receptors (regardless of conformation). As a consequence, a predicted result of bioassays on this series of scaffold models is that of a universal lack of binding.

Such predictions were largely confirmed, as shown in **Table 1b**, supporting the hypothesis that any binding and activity previously observed in the library of disulfide-rich analogues was predominantly due to inclusion of the active pharmacophore sequence [His-Phe-Arg-Trp] and subsequent backbone cyclization. The exceptions of MM7, MM8, MM9, and MM14 may have occurred due to alteration of a segment of the peptide which produced mimicry of the beta-turn structure of ligands for melanocortin receptors, but such conclusions should be verified through repeated assays as well as a more detailed structural (NMR) analysis.

James Cain's Small Molecules

As previously mentioned, small molecules possess the advantage of lessened susceptibility to degradation by proteases in comparison to their peptide analogue counterparts; consequently, medicinal dosages of small molecules to are presumed to be smaller than those of peptide chemotherapeutics. This library of small molecules was derived from a core template achieved via the coupling of L-proline and L-phenylalanine, followed by cyclization and reduction (**Figure 4**). Acylation of the core template with functional groups provided the basis for generation of this library and other similar compounds.

[50] Li, J. et al. *Molecular and Cellular Proteomics*. **2007**, *6*, 882-894.
[51] Craik, D.J. *Toxins* **2012**, *4*, 139-156.
[52] Daly, N.L. *European Biophysics Journal* **2011**, *40*, 367-368.

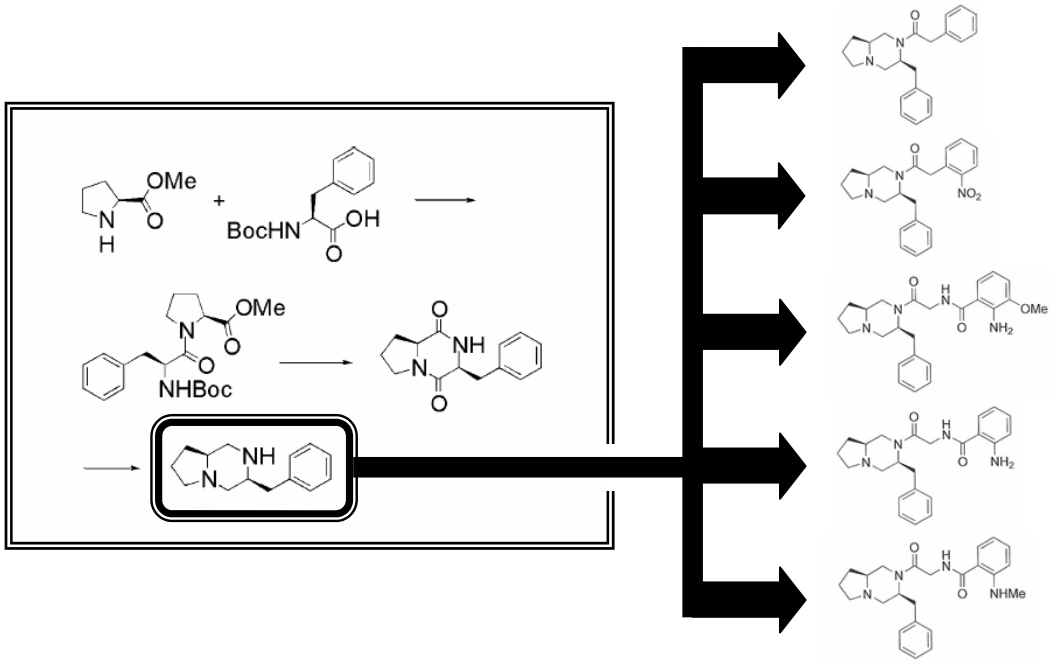

Figure 4. The construction of a bicyclic diamine core template from the amino acids L-proline and L-phenylalanine provides the starting point for the synthesis of a wide range of small molecules. (Cain, J.P. et al. *Bioorganic & Medicinal Chemistry Letters*, **2006**, *16*, 5462-5467.)

The affinities and efficacies of the small molecule mimetics are presented in **Table 2**. JPC 5140 was identified as a selective partial antagonist of hMC1R; its IC_{50} is at least two orders of magnitude lesser at that target than at any other receptor, and this suggests that there may exist a binding site distinct from the orthosteric one that this compound is binding to. Similarly, JPC 6007 was observed to be a selective, allosteric inhibitor of hMC3R; again, its IC_{50} is approximately two orders of magnitude lesser at this receptor relative to the others. Finally, JPC 8029, JPC 8042, and JPC 9034 appear to be selective allosteric inhibitors of hMC5R; the IC_{50} values of JPC 8029 and JPC 8042 are at least two orders of magnitude lesser at this target in comparison to the others, while the IC_{50} value of JPC 9034 is approximately one order of magnitude lesser.

Allosteric ligands have been of particular interest in drug discovery for their ability to exert exquisitely controlled modulation on GPCRs. Because they act in concert with endogenous ligands, allosteric modulators conform more closely to physiology than synthetic orthosteric ligands, and may require lower dosages as well as result in fewer undesirable side effects. Furthermore, they possess the potential to be exceptionally selective, as allosteric binding sites are less subject to evolutionary conservation compared to orthosteric sites[53]. These findings thereby provide an opportunity to further investigate the nature of modulation employed by these apparently allosteric ligands.

Because small molecule mimetics are naturally much more compact and constrained in structure than peptide analogues, this discussion will involve an analysis of the effects of certain functional groups and their positions on the core template at each receptor. Ultimately, the mimetic should

[53] Christopoulos, A. et al., *Biochemical Society Transactions* **2004**, *32*, 873.

imitate the β-turn of an active pharmacophore such as the tetrapeptide [His-Phe-Arg-Trp] of endogenous α-MSH, or [His-D-Phe-Arg-Trp] of MT-II if it is to possess similar bioactivity (**Figure 5**).

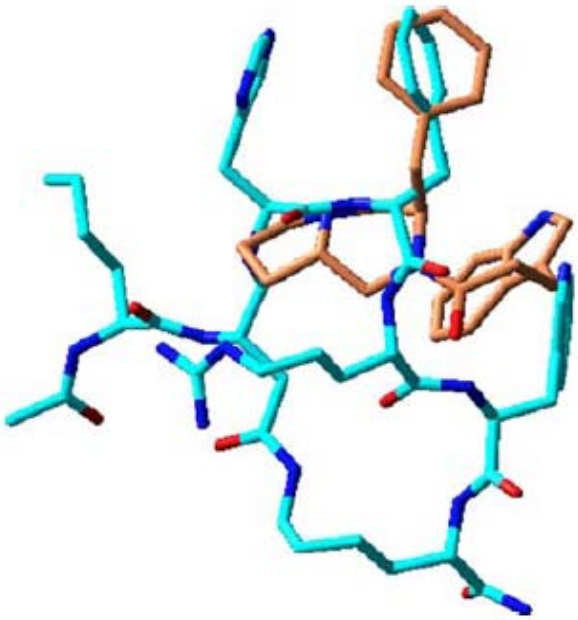

Figure 5. Superimposition of a functionalized analogue derived from the core template (orange) and the superpotent, non-selective agonist MT-II (blue). Analogues that possess the most overlap with MT-II are predicted to be the most biologically active. (Cain, J.P. et al. *Bioorganic & Medicinal Chemistry Letters*, **2006**, *16*, 5462-5467.)

hMC1R

The position of substitution on the functionalized phenyl linked to the diamine core template is significant; this is illustrated by the 100-fold decrease in binding affinity when the phenyl was ortho-substituted, as in JPC 5140, as opposed to para-substituted, as in JPC 6007.

Next, the molecules JPC 8029, JPC 8042, and JPC 9011 suggested that the inversion of the stereochemistry (*S* to *R*) of the chiral carbon joining the two heterocycles of the core template decreases binding affinity; the IC_{50} values of these molecules were relatively large in the micromolar range. Furthermore, the IC_{50} value of JPC 9011 was noticeably outsized at 7000 nM, suggesting that the inversion of the configuration (*S* to *R*) at the chiral carbon associated with the benzyl group of the core template also decreases binding affinity.

The increase in linker length as illustrated by JPC 6072 appeared to lower binding affinity as well.

Because low binding affinity is usually an indicator of low activity and signaling response, it was to some extent expected that the corresponding effectivities of these small molecules were not measurable to any considerable degree[54]. The exception was JPC 5140, which possessed a relatively high binding affinity.

[54] Erhardt, Paul. *Pharmacology: Principles and Practice*, **2009**, 475-560.

In general, these results suggest that in order to achieve successful binding at hMC1R, a small molecule synthesized from this particular template should possess an *S*-configuration at both chiral centers on the diamine core, and a para-substituted group on the functionalized phenyl associated to the core by a relatively short linker.

hMC3R

The significance of the position of substitution on the functionalized phenyl linked to the diamine core template appeared to be reversed from that of hMC1R; para-substitution is no longer favored over ortho-substitution, as illustrated by 200-fold decrease in binding affinity from JPC 6007 to JPC 5140.

However, the preference for *S*-stereochemistry appeared to hold from hMC1R to hMC3R; the molecules JPC 8029 and JPC 8042 exhibited comparable IC_{50} values across hMC1R and hMC3R in the low-micromolar range. In addition, the relatively large and heavily functionalized molecule JPC 6072 exhibited the largest IC_{50} value, despite its conformation to the preferred *S*-stereochemistry; this suggested that the binding pocket may better accept ligands of lesser steric hindrance or functionalities than this.

Interestingly, JPC 9034 was characterized by an IC_{50} value one order of magnitude smaller than that of JPC 6072, despite that the two molecules possessed virtually identical structures. The reason for this may be the methyl group associated with the secondary amine that was present on the functionalized phenyl in JPC 9034; this structure, which is ortho-substituted, may have offset the shared factors that caused JPC 6072 to possess low binding ability. Conversely, the tri-substituted phenyl of JPC 6072 may have hindered binding affinity.

Again, as seen in hMC1R, the small molecules were characterized by little to no effectivity. (The exception was JPC 9011, which requires further investigation.)

Overall, these results suggest that in order to successfully bind hMC3R, a ligand synthesized from this template should be of a relatively small size and possess a di-, ortho-substituted phenyl associated to the diamine core by a relatively small linker.

hMC4R

No small molecules were able to effectively bind hMC4R, with the exception of JPC 9034, which possessed an IC_{50} value of 476 nM and a binding efficiency of 100%. However, because this was the only molecule that achieved effective binding and there exist no models for comparison, it is not possible to infer the reason why JPC 9034 in particular was successful in binding hMC4R, from a comparative structural viewpoint.

The corresponding effectivities of the small molecules at hMC4R were not measurable due to inability to bind. Though JPC 9034 bound the target receptor, it also produced no measurable secondary messenger response; it was therefore identified as an antagonist at hMC4R.

hMC5R

The most readily observed trend in the binding of the small molecules to hMC5R was that the presence of a methoxy group on the phenyl group linked to the core template greatly decreased binding affinity, in the para-substituted configuration more so than the ortho- or meta-substituted ones. The para-substituted JPC 5140 possessed an outsized IC_{50} value of 5720 nM; the ortho- and meta-substituted JPC 6007 and JPC 6072 were similar and possessed IC_{50} values of approximately 1500 nM.

Second, it appears that the stereochemistry of the chiral carbon joining the two heterocycles of the template is not of critical importance; rather, the configuration of the carbon associated with

the benzyl group of the diamine core takes precedence. JPC 8042 and JPC 9011 are virtually identical molecules, but the inversion of this particular center in JPC 9011 (*S* to *R*) produced a 2000-fold decrease in binding affinity.

While these small molecules bound hMC5R with some efficiency, none induced a significant, measurable response in the target cell; they were thereby classified as antagonists of hMC5R.

Joel Nyberg's Cyclic Peptides

Covalent cyclization of peptides can be achieved in several ways; these involve bridging two side chains, two backbone residues, or one side chain to either the N- or C-terminus[55]. This library features peptides that exhibit lactam bridges between two side chains, as well as the active core pharmacophore of the potent universal melanocortin receptor antagonist SHU-9119, [His-D-Nal(2')-Arg-Trp] (**Figure 6**). The scaffold from which these peptides were based resembles that of SHU-9119 (as well as MT-II), but features additional glycine, lysine, and proline residues external to the cyclized segment. As previously discussed, cyclization imparts several benefits to the affinity of the ligand by reducing the degrees of freedom in the molecule and constraining the pharmacophore to more bioactive conformations[56, 57].

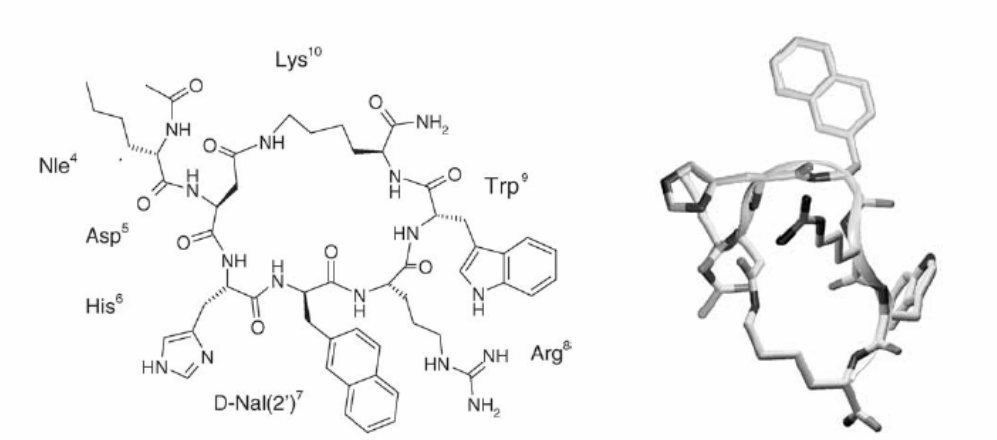

Figure 6. Substitution of the phenylalanine residue in the α-MSH pharmacophore framework with a bulky, lipophilic D-Nal(2') obtains the antagonistic character of the potent α-MSH analogue, SHU 9119. (Cai, M. et al. *Peptides* **2005**, *26*, 1482.)

The affinities and efficacies of the cyclized peptides are presented in **Table 3**. All of the peptide analogues exhibited exceptional binding affinities for hMC1R, possessing IC_{50} values that did not exceed 10 nM; the associated binding efficiencies all exceeded 90%. Because these analogues generally induced a strong response in activity with similarly undersized EC_{50} values, they were identified as full agonists of hMC1R.

[55] Fung, S. et al. Current Opinion in Chemical Biology **2005**, *9*, 352-358.
[56] Fung, S. et al. Current Opinion in Chemical Biology **2005**, *9*, 352-358.
[57] Daly, N.L. *European Biophysics Journal* **2011**, *40*, 367-368.

Interestingly, the behavior of the peptide analogues at the hMC4R subtype is fairly parallel to that in the presence of hMC1R, if on a less efficient scale. All analogues exhibited reasonably effective binding character, possessing IC_{50} values that did not exceed one micromolar and binding efficiencies that exceeded 65%. All of the analogues also induced a considerable, if not full, response in the target cell and possessed EC_{50} values that did not exceed 550 nM. Consequently, they were classified as partial agonists of hMC4R.

At the receptor subtypes hMC3R and hMC5R, moderate to exceptional binding was observed (for hMC3R, IC_{50} values did not exceed 50 nM and the corresponding binding efficiencies all exceeded 95%, and for hMC5R, IC_{50} values that did not exceed the 2270 nM and binding efficiencies that exceeded 85%) with a reversed effect on receptor activity than that seen in hMC1R and hMC4R: no appreciable secondary messenger response was elicited at either hMC3R or hMC5R, and as a result, all analogues were considered antagonists of those receptor subtypes.

Conclusions

With this study, the application of disulfide-rich cyclic knot peptides in drug discovery appears to possess lucrative potential. It was determined that insertion of an active pharmacophore into the otherwise inactive framework of SFTI-1 produced agonistic results, depending on the site of incorporation; this establishes the opportunity for the assimilation of cyclic knots as suitable scaffolds in novel drug design. Beyond this discovery, a number of receptor-specific compounds were identified. PC2, PC3, and PC24b were identified as hMC1R-selective agonists, and PC19c as an hMC1R-selective antagonist; PC20a was identified as an hMC3R-selective agonist; PC11b, PC19b exhibited exceptional affinity for hMC4R with IC_{50} values in the low- to mid-nanomolar range and produced partial selective antagonism when bound, and PC30 was identified as a full antagonist of hMC4R; and finally, PC16b and PC18a exhibited selective antagonism of hMC5R.

Supplementary assays of a series of linear molecular scaffolds based on the naturally occurring peptides SFTI-1, odorranain-b1, and MCoTI-II have provided preliminary evidence that the binding and activity previously observed in this library of disulfide-rich, *N*-methylated analogues was largely due to inclusion of the active pharmacophore sequence [His-Phe-Arg-Trp] and subsequent backbone cyclization. These data will require repeated assays, and will be supplemented with adenylate cyclase activity assays next semester.

Several of James Cain's small molecules possess therapeutically relevant selectivity profiles. First, JPC 5140 was determined to be a selective partial antagonist of hMC1R. Second, JPC 6007 appears to be a selective, allosteric inhibitor of hMC3R; again, its IC_{50} is approximately two orders of magnitude lesser at this receptor relative to the others. Finally, JPC 8029, JPC 8042, and JPC 9034 appear to be selective allosteric inhibitors of hMC5R; the IC_{50} values of JPC 8029 and JPC 8042 are at least two orders of magnitude lesser at this target in comparison to the others, while the IC_{50} value of JPC 9034 is approximately one order of magnitude lesser.

All of Joel Nyberg's cyclized peptides exhibited either full agonistic or full antagonistic qualities at two of the four receptor subtypes; however, a peptide which was selective for a single receptor was not identified.

These assays provide an important starting point for continued modification of these models. Future directions may include the optimization of the selective and therapeutically relevant compounds.

Acknowledgements

This research was supported by the US Public Health Service (DK17420), National Institutes of Health (DA06248), and the Undergraduate Biology Research Program at the University of Arizona through HHMI (52003749).

References

Barbeta, B.L.; Marshall, A.T.; Gillon, A.D.; Craik, D.J.; Anderson, M.A. Plant cyclotides disrupt epithelial cells in the midgut of lepidopteran larvae. *Proceedings of the National Academy of Sciences of the United States of America.* **2008**, *105*, 1222.

Cai, M.; Mayorov, A.V.; Ying, J.; Stankova, M.; Trivedi, D.; Cabello, C.; Hruby, V.J. Design of novel melanotropin agonists and antagonists with high potency and selectivity for human melanocortin receptors. *Peptides.* **2005**, *26*, 1481-1485.

Cai, M.; Nyberg, J.; Hruby, V.J. Melanotropins as drugs for the treatment of obesity and other feeding disorders: potential and problems. *Current Topics in Medicinal Chemistry.* **2009**, *9*, 554-563.

Cain, J.P.; Mayorov, A.V.; Cai, M.; Wang, H.; Tan, B.; Chandler, K.; Lee, Y.; Petrov, R.R.; Trivedi, D.; Hruby, V. Design, synthesis, and biological evaluation of a new class of small molecule peptide mimetics targeting the melanocortin receptors. *Bioorganic & Medicinal Chemistry Letters.* **2006**, *16*, 5462–5467.

Chatterjee, J.; Ovadia, O.; Zahn, G.; Marinelli, L.; Hoffman, A.; Gilon, C.; Kessler, H. Multiple N-methylation by a designed approach enhances receptor selectivity. *Journal of Medicinal Chemistry.* **2007**, *50*, 5878-5881.

Christopoulos, A.; May, L.T.; Avlani, V.A.; Sexton, P.M. G-protein-coupled receptor allosterism: the promise and the problem(s). *Biochemical Society Transactions.* **2004**, *32*, 873-877.

Clark, R.J.; Akcan M.; Kaas, Q.; Daly, N.L.; Craik, D.J. Cyclization of conotoxins to improve their biopharmaceutical properties. *Toxicon.* **2012**, *59*, 446-455.

Clark, R.J.; Fischer, H.; Dempster, L.; Daly, N.L.; Rosengren, K.J.; Nevin, S.T.; Meunier, F.A.; Adams, D.J.; Craik, D.J. Engineering stable peptide toxins by means of backbone cyclization: Stabilization of the alpha-conotoxin MII. *Proceedings of the National Academy of Sciences of the United States of America.* **2005**, *102*, 13767-13772.

Clark, R.J.; Jenson, J.; Nevin, S.T.; Callaghan, B.P.; Adams, D.J.; Craik, D.J. The engineering of an orally active conotoxin for the treatment of neuropathic pain. *Angewandte Chemie-International Edition.* **2010**, *49,* 6545 –6548.

Craik, D.J. Host-defense activities of cyclotides. *Toxins.* **2012**, *4*, 139-156.

Cody, W.L.; He, J.X.; Reily, M.D.; Haleen, S.J.; Walker, D.M.; Reyner, E.L.; Stewart, B.H.; Doherty, A.M. Design of a potent combined pseudopeptide endothelin-A/endothelin-B receptor antagonist, Ac-DBhg(16)-Leu-Asp-Ile-[NMe]Ile-Trp(21) (PD 156252): Examination of its pharmacokinetic and spectral properties. *Journal of Medicinal Chemistry.* **1997**, *40*, 2228-2240.

Cone, R.D. Anatomy and regulation of the central melanocortin system. *Nature Neuroscience.* **2005**, *8*, 571-78.

Daly, N.L.; Rosengren, K.J.; Henriques, S.T.; Craik, D.J. NMR and protein structure in drug design: Application to cyclotides and conotoxins. *European Biophysics Journal* **2011**, *40*, 359-370.

Daly, N.L.; Rosengren, K.J.; Craik, D.J. Discovery, structure and biological activities of cyclotides. *Advanced Drug Delivery Reviews*. **2009**, *61*, 918–930.

Dawson, P.E.; Muir, T.W.; Clark-Lewis, I.; Kent, S.B.H. Synthesis of proteins by native chemical ligation. *Science*. **1994**, *266*, 776-779.

Doedens, L.; Opperer F.; Cai, M.; Beck J.G.; Dedek, M.; Palmer, E.; Hruby V.J.; Kessler, H. Multiple N-methylation of MT-II backbone amide bonds leads to melanocortin receptor subtype hMC1R selectivity: pharmacological and conformational studies. *Journal of the American Chemical Society*. **2010**, *132*, 8115-8128.

Erhardt, P. Chapter 19: Drug Discovery. *Pharmacology: Principles and Practice*. Oxford: Elsevier Academic. **2009**, 475-560.

Fairlie, D.P.; Abbenante, G.; March, D.R. Macrocyclicpeptidomimetics forcing peptides into bioactive conformations. *Current Medicinal Chemistry*. **1995**, *2*, 654-686.

Fung, S.; Hruby, V.J. Design of cyclic and other templates for potent and selective peptide alpha-MSH analogues. *Current Opinion in Chemical Biology*. **2005**, *9*, 352-358.

Korsinczky M.L.J.; Clark, R.J.; Craik, D.J. Disulfide bond mutagenesis and the structure and function of the head-to-tail macrocyclic trypsin inhibitor SFTI-1. *Biochemistry* **2005**, *44*, 1145-1153.

Li, J.; Xu, X.; Xu, C.; Zhou, W.; Zhang, K.; Yu, H.; Zhang, Y.; Zheng, Y.; Rees, H.; Lai, R.; Yang, D.; Wu, J. Anti-infection peptidomics of amphibian skin. *Molecular and Cellular Proteomics*. **2007**, *6*, 882-894.

Lovelace, E.S.; Gunasekera, S.; Alvarmo, C.; Clark, R.J.; Nevin, S.T.; Grishin, A.A.; Adams, D.J.; Craik, D.J.; Daly, N.L. Stabilization of α-conotoxin AuIB: influences of disulfide connectivity and backbone cyclization. *Antioxidants and Redox Signaling*. **2010**, *14*, 87-95.

Lundstrom, K. An overview on GPCRs and drug discovery: structure-based drug design and structural biology on GPCRs. *Methods in Molecular Biology*. **2009**, *552*, 51-66.

McIntosh, J.M.; Jones, R.M. Cone venom—from accidental stings to deliberate injection. *Toxicon*. **2005**, *39*, 1447-1451.

Patil, R.; Das, S.; Stanley, A.; Yadav, L.; Sudhakar, A.; Varma, A.K. Optimized hydrophobic interactions and hydrogen bonding at the target-ligand interface leads the pathways of drug-designing. *PLoS ONE*. **2010**, *5*. Web.

Pierce, K.L.; Premont, R.T.; Lefkowitz, R.J. Seven-transmembrane receptors. *Nature Reviews Molecular Cell Biology*. **2002**, *3*, 639-650.

Sangalli, L.; Bortolotti, A.; Jiritano, L.; Bonati, M. Cyclosporine pharmacokinetics in rats and interspecies comparison in dogs, rabbits, rats, and humans. *Drug Metabolism and Disposition.* **1988**, *16*, 749-753.

Smith, J.M.; Hows J.M.; Gordon-Smith, E.C. Stability of Cyclosporin-A in Human-Serum. *Journal of Clinical Pathology.* **1983**, *36*, 41-43.

Stenkamp, R.E. Alternative models for two crystal structures of bovine rhodopsin. *Acta Crystallographica Section D Biological Crystallography.* **2008**, *64*, 902-04.

Takeda, S.; Kadowaki, S.; Haga, T.; Takaesu, H.; Mitaku, S. Identification of G protein-coupled receptor genes from the human genome sequence. *FEBS Letters.* **2002**, *520*, 97-101.

Tikhonova, I.G.; Costanzi, S. Unraveling the structure and function of G protein-coupled receptors through NMR spectroscopy. *Current Pharmaceutical Design.* **2009**, *15*, 4003-016.

Voisey, J.; Carroll, L.; van Daal, A. Melanocortins and their receptors and antagonists. *Current Drug Targets.* **2003**, *4*, 586-597.

Wang, H.; Yu, Z.; Hu, Y.; Li, F.; Liu, L.; Zheng, H.; Meng, H.; Yang, S.; Yang, X.; Liu, J. Novel antimicrobial peptides isolated from the skin secretions of Hainan odorous frog, Odorrana hainanensis. *Peptides.* **2012**, *35*, 285-290.

Yeagle, P.L.; Albert, A.D. G-protein coupled receptor structure. *Biochimica Et Biophysica Acta (BBA) – Biomembranes.* **2007**, *1768*, 808-24.